REPORT DOCUMENTATION PAGE

Form Approved

OMB No. 0704-0188

PLEASE DO NOT RETURN YOUR FORM TO THE ABOVE ADDRESS.

1. REPORT DATE *(DD-MM-YYYY)*	2. REPORT TYPE	3. DATES COVERED *(From - To)*
14-12-1999	Final	1 Dec 95 – 30 Nov 97

4. TITLE AND SUBTITLE

The Synthesis, Processing, Deformation and Failure of Superplastic Nanocrystalline Ceramic Composites

5a. CONTRACT NUMBER

F49620-96-1-0022

5b. GRANT NUMBER

5c. PROGRAM ELEMENT NUMBER

6. AUTHOR(S)

Dr. Atul H. Chokshi

5d. PROJECT NUMBER

5e. TASK NUMBER

5f. WORK UNIT NUMBER

7. PERFORMING ORGANIZATION NAME(S) AND ADDRESS(ES)

Indian Institute of Science
Department of Metallurgy
Bangalore 56012
India

8. PERFORMING ORGANIZATION REPORT NUMBER

N/A

9. SPONSORING/MONITORING AGENCY NAME(S) AND ADDRESS(ES)

AOARD
UNIT 45002
APO AP 96337-5002

10. SPONSOR/MONITOR'S ACRONYM(S)

AOARD

11. SPONSOR/MONITOR'S REPORT NUMBER(S)

AOARD-954003

12. DISTRIBUTUION/AVAILABILITY STATEMENT

Approved for public release; distribution is unlimited.

13 SUPPLEMENTARY NOTES

14. ABSTRACT

Commercially available nanocrystalline 3 mol% yttria stabilized tetragonal zirconia powders with a crystallite size of <40 nm were processed using a colloidal technique. Essentially, the powders were dispersed in de-ionized water, and the pH of the solution was adjusted to ~2 to disperse the powders. The solution was ultrasonicated and then pressure filtered to produce a green body with a relative density of ~50%. The densification and grain growth characteristics of zirconia were examined during the free sintering and sinter-forging (sintering with the application of a compressive uniaxial stress without any lateral constraints) at temperatures in the range of ~1600 to 1750K. It was demonstrated that it is possible to produce fully dense compacts with a grain size of ~175 nm using this technique. During sinter-forging, both densification and creep processes occur simultaneously; the measurement of density and axial strain enable to separation of the kinetics of the two processes. It was shown that deformation during densification occurs by an identical process as in fully dense materials (mainly grain boundary sliding). Furthermore, the differences in the stress exponents for creep and densification indicated that densification was not controlled directly by deformation.

15. SUBJECT TERMS

Nanocrystalline, Compressive Uniaxial Stress, Ultrasonicated, Sinter-Forging

16. SECURITY CLASSIFICATION OF:			17. LIMITATION OF ABSTRACT	18. NUMBE OF PAGES	19a. NAME OF RESPONSIBLE PERSON
a. REPORT	b. ABSTRACT	c. THIS PAGE			Thomas Kim
U	U	U	UU	22	19b. TELEPHONE NUMBER *(Include area code)* +81-3-5410-4409

Standard Form 298 (Rev. 8/98)
Prescribed by ANSI Std. Z39.18

Synthesis, Processing, Deformation and Failure of Superplastic Nanocrystalline Ceramic Composites

Final Report for period 1 Dec 95 -30 Nov 97

Department of Metallurgy
Indian Institute of Science
Bangalore 560 012
India

Grant No. F49620-96-1-0022

PI's: Drs. Atul H. Chokshi and Vikram Jayaram

OBJECTIVE

The present investigation was designed to study the synthesis, processing and high temperature mechanical properties of nanocrystalline ceramics and ceramic composites.

Research Accomplishments and New Findings

Colloidal Processing of Nanocrystalline Zirconia (details in Appendix 1)

Commercially available nanocrystalline 3 mol% yttria stabilized tetragonal zirconia powders with a crystallite size of <40 nm were processed using a colloidal technique. Essentially, the powders were dispersed in de-ionized water, and the pH of the solution was adjusted to ~2 to disperse the powders. The solution was ultrasonicated and then pressure filtered to produce a green body with a relative density of ~50%. The densification and grain growth characteristics of zirconia were examined during the free sintering and sinter-forging (sintering with the application of a compressive uniaxial stress without any lateral constraints) at temperatures in the range of ~1600 to 1750 K.

It was demonstrated that it is possible to produce fully dense compacts with a grain size of ~175 nm using this technique. During sinter-forging, both densification and creep processes occur simultaneously; the measurement of density and axial strain enable to separation of the kinetics of the two processes. It was shown that deformation during densification occurs by an identical process as in fully dense materials (mainly grain boundary sliding). Furthermore, the differences in the stress exponents for creep and densification indicated that densification was not controlled directly by deformation.

Colloidal Processing of Nanocrystalline Alumina-Yttria Composites (details in Appendix 2)

Commercial grades of nanocrystalline alumina (<70 nm) and yttria were utilized for this project. The alumina powders were processed in a manner similar to that utilized above for zirconia. For alumina-yttria composites, the alumina and yttria powders were dispersed separately at a pH of ~2, then mixed in the appropriate proportion, ultrasonicated and flocced

to limit segregation of particles. The flocced slurry was then pressure filtered, and densification in such compacts was examined during free sintering and sinter-forging.

In view of the very limited solubility of yttria in alumina, as anticipated the yttria powders reacted with the alumina powders during the heating up from room temperature to 1550 K, so that the results related essentially to alumina-YAG composites. There was significant grain growth during the final stages of densification in high purity alumina, so that the final grain sizes in fully dense samples were typically in the range of ~2 μm. The presence of YAG retarded densification considerably, but it was possible to obtain fully dense alumina-YAG composites by sinter-forging. The YAG particles also hindered grain growth so that the final grain sizes in the alumina-YAG composites were in the range of ~400 nm.

Synthesis/Processing of Amorphous and Nanocrystalline Alumina-Zirconia Composites by Spray Pyrolysis (details in Appendix 3)

Spray pyrolysis of solutions of nitrates has been used to produce amorphous particles of zirconia-40 mol% alumina solid solutions. When these agglomerates were subjected to high pressure compaction (500-750 MPa) at low temperatures (500-650 C), they displayed large regions of surprisingly high density. By sedimenting out coarse particulate, it was found possible to produce homogeneously dense (96%) compacts while retaining the amorphous structure. This is the first reported synthesis, in bulk form, of non-crystalline material in the zirconia-alumina system. In-situ monitoring of the consolidation of the powders reveals that significant plastic flow takes place. Powder pycnometry indicates that the amorphous solid has a density of about 3.3 g/cc, which is about 2/3 of the value expected from the stable phases in this composition. It seems likely that the increased plastic response is an off-shoot of the larger inter-ionic spacings and non-equilibrium coordination in the glass

relative to those that exist in the crystalline compounds. Residual volatile species are less than 1 wt%, but could conceivably stabilise the amorphous structure.

The crystallisation of the densified compacts has made it possible to produce nanostructured materials in pellet form, without the need to use nano-sized powders. Heat treatments in the range of 900-1000 C produce tetragonal zirconia and gamma alumina with grain sizes in the range of 5-8 nm, while temperatures above 1100 C result in alpha alumina and a mixed tetragonal/monoclinic zirconia with a microstructural scale of 50-300 nm. The coarsest microstructures (300 nm) are stable for up to 2 hours at 1400 C.

Processing of Nanocrystalline Alumina-Zirconia Composites with SiC Whiskers (details in Appendix 3)

The densification of alumina rich glasses (20 mole % ZrO2) was accomplished under the same conditions as described above. In addition, composites were prepared with about 9 wt % SiC (< 3 microns) that was incorporated in the matrix by spray-decomposing a suspension of SiC in the precursor nitrate solution. It was shown that such a composite could be densified at 650 C , 750 MPa to 99% density, indicating that the densification of the amorphous matrix was little impeded by the presence of rigid inclusions. It is clear that the crystallisation of such a material offers the possibility of producing SiC reinforced alumina-zirconia with controlled, nanocrystalline matrices at low temperatures without the need for inert atmospheres.

Potential Areas for Further Studies

The following aspects that emerged from the present investigation are potential areas for further research studies.

(1) Fabrication of amorphous pellets and a study of their deformation behaviour under constant strain rate and constant stress,

(2) The study of densification of amorphous powder aggregates during hot pressing and sinter-forging,

(3) The production of nanocrystalline two-phase mixtures of zirconia and alumina and their superplastic behavior

(4) Modification of microstructure to produce a more creep resistant composite, after superplastic deformation, and the high temperature deformation behavior of the composite in the modified form, and

(5) the extension of low temperature densification to other systems in which amorphous/metastable phases may be induced to form.

Personnel Supported

In addition to the PI's, Mr. A.S. Gandhi, a graduate student working towards his Ph.D.

Publications

1. The Densification, Superplastic Deformation and Fracture Characteristics of a 3 mol% Yttria Stabilized Zirconia, A.H. Chokshi, Progress in Advanced Materials and Mechanics (Wang Tzuchiang and Tsu-Wei Chou, eds.). Peking University Press, China (1996).
2. A.S. Gandhi, V. Jayaram and A.H. Chokshi, :Phase Evolution and Densification of Spray Pyrolysed ZrO_2-Al_2O_3 Powders," Materials Science Forum (A.H. Chokshi, ed), 243-245, 227-232 (1997).
3. S. Krishnamurthy and A.H. Chokshi, "High Temperature Deformation and Densification in Alumina-Yttria Composites," Materials Science Forum (A.H. Chokshi, ed.), 243-245, 369-374 (1997).
4. A.S. Gandhi, V. Jayaram and A.H. Chokshi, "Low Temperature Consolidation of Metastable Phases in Alumina-Zirconia," Recent Advances in Metallurgical Processes (D.H. Sastry, E.S. Dwarkadasa and S. Subramanian, eds.), vol. 1, pp. 727-731. New Age Publishers, Bangalore, India (1997).
5. The Significance of Diffusional Flow in Ultra-Fine Grained Materials, S. Shah and A.H. Chokshi, Colloids and Surfaces A133, 57-61 (1998).
6. A.S. Gandhi, V. Jayaram and A.H. Chokshi, "Dense Amorphous Zirconia-Alumina by Low Temperature Consolidation of Spray Pyrolysed Powders," Journal of the Amercian Ceramic Society (in press).

More technical data and figures are included in Appenidx 1, 2 and 3 which are copies of the references 1, 3 and 6 above.

Appendix A1

ed. Wang Tzuchiang + Tan - Wei chou, Peking Univ. Press (1996).

Progress in Advanced Materials and Mechanics

THE DENSIFICATION, SUPERPLASTIC DEFORMATION AND FRACTURE CHARACTERISTICS OF A 3 MOL% YTTRIA STABILIZED ZIRCONIA

Atul H. Chokshi
(Department of Metallurgy, Indian Institute of Science, Bangalore 560 012, India)

ABSTRACT: Following the early report of a superplastic elongation of >100% in a 3 mol% yttria stabilized zirconia in 1986 by Wakai and colleagues from Japan; there have been numerous investigations of the mechanical behavior of superplastic zirconias and their allied composites. This report provides a broad overview of the deformation, densification, grain growth and fracture characteristics of a superplastic 3YTZ; all of these phenomena are linked by the common thread of diffusion.

KEY WORDS: superplasticity, zirconia, densification, grain growth, fracture

I. INTRODUCTION

There has been considerable activity in the area of superplasticity in ceramics following the spectacular report by Wakai *et al.* [1] of an elongation of >100% in a 3 mol% yttria stabilized tetragonal zirconia (3YTZ), which is a commercially significant ceramic. Subsequently, there have been numerous studies on the mechanical characteristics of the material, and these have been summarized in many reviews on the topic [2-4].

There are two important microstructural changes accompanying superplastic deformation - grain growth and cavitation; all of these are thermally activated processes dependent on diffusion. In contrast to metallic superplastic alloys that are made conventionally using the ingot metallurgy route, with an appropriate thermo-mechanical treatment, bulk ceramics are usually produced from powders, and the densification process also involves diffusion.

The present report provides a broad overview of superplastic deformation, densification, grain growth and fracture in a 3 mol% yttria stabilized zirconia.

II. SUPERPLASTIC DEFORMATION

The mechanical characteristics of superplastic materials can be described by an equation of the following form:

$$\dot{\varepsilon} = \frac{ADGb}{kT}\left(\frac{b}{d}\right)^{p}\left(\frac{\sigma}{G}\right)^{n} \qquad (1)$$

where $\dot{\varepsilon}$ is the strain rate, A is a dimensionless constant, D is the appropriate diffusivity, G is the shear modulus, b is the magnitude of the Burgers vector, k is Boltzmann's constant, T is the absolute temperature, d is the grain size, p is the inverse grain size exponent, σ is the stress and n is the stress exponent. The diffusion coefficient may be expressed as $D=D_0 \exp(-Q/RT)$, where D_0 is a frequency term, Q is the activation energy for the rate controlling process and R is the gas constant.

Early studies on the superplastic 3YTZ revealed important discrepancies in the value of the stress exponent, with values of n being close to either 2 or 3 [2-4]. Carry [5] has suggested that these differences arise from minor variations in the impurity contents of the materials studied, such that material with higher and lower impurity contents exhibit stress exponents of ~2 or ~3, respectively.

A more recent detailed study on the constant stress compression behavior of 3YTZ indicated that a material with a given composition can exhibit both n~2 and n~3 behavior depending on the experimental conditions used: thus, for a given grain size and temperature, there is a transition from a stress exponent of ~2 at high stresses to ~3 at low stresses [3,6,7]. The experimental data are shown in Fig. 1 in the form of a logarithmic plot of strain rate versus stress for compression experiments on 3YTZ together with the data obtained in tension on a 2YTZ [8]; the slopes of the curves define the stress exponent for creep. It is clear from an inspection of the data that there is a transition from n~2 at high stresses to n~3 at low stresses. Additional experiments on 3YTZ indicated that the stress for transition from n~3 to n~2, σ_t, decreases with an increase in grain size [3,7].

In view of the observed changes in n with stress and grain size, it is necessary to exercise caution in evaluating the rate controlling parameters for superplastic deformation. Thus, for example, in order to obtain the value of the inverse grain size exponent p, it is necessary to ensure that the data are being evaluated under conditions where σ, T, n and Q are identical. The wide dispersion in the values of p and Q reported in the literature may be a consequence of an appropriate lack of critical consideration of these factors. A careful examination of the data in 3YTZ indicated that creep with n~3 is associated with an activation energy of ~550 kJ mol^{-1}[7].

Based on these observations, it was suggested that the transition from n~2 to n~3 is controlled by the impurity content of the material such that σ_t is displaced to lower values for materials with higher impurity content (equivalent to a coarser grain size). The experimentally observed decrease in stress exponent may be rationalized using the concepts of (a) operation of two sequential processes, in which the slower process is rate controlling, or (b) the presence of a threshold stress, so that the creep rate decreases continuously as the applied stress approaches a threshold value [3,6,7].

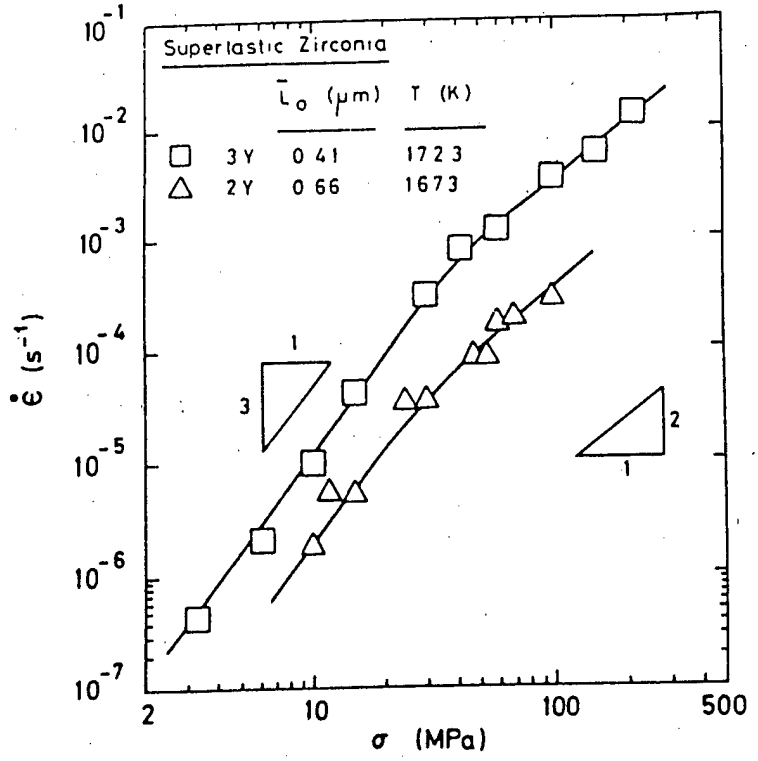

Fig. 1 Variation in strain rate with stress for a yttria stabilized zirconia containing 3 mol% (2Y) and 2 mol% (3Y) yttria [6,8].

III. DENSIFICATION PROCESSES

In contrast to metallic alloys, bulk ceramic components are usually manufactured using powder processing techniques, which involve sintering to produce fully dense materials. The removal of voids in such compacts is usually accomplished by diffusion related processes. Sinter-forging, which involves the application of a uniaxial compressive load without any lateral constraints, is an interesting technique for studying the densification characteristics of ceramics. It is possible to simultaneously characterize both densification and creep by measurements of the axial strain and transverse strain (or density) since shape change is such experiments occurs due to both the removal of voids and plastic deformation.

A detailed study was undertaken recently to characterize the densification characteristics of 3YTZ [9]. Figure 2 illustrates some of the experimental data obtained in the form of the variation with imposed stress the (a) porosity (φ) compensated strain rate (left axis) and (b) densification rate , $\dot{\rho}$, (right axis). Also included in Fig. 2 are the experimental datum points obtained for the creep rate in fully dense (φ=0) 3YTZ. The experimental results indicated that during sinter-forging $\dot{\varepsilon} \propto \exp(\alpha\phi)$ with the constant α=19, for a fixed stress, temperature and grain size; consequently, it is possible to normalize the creep rate for differences in

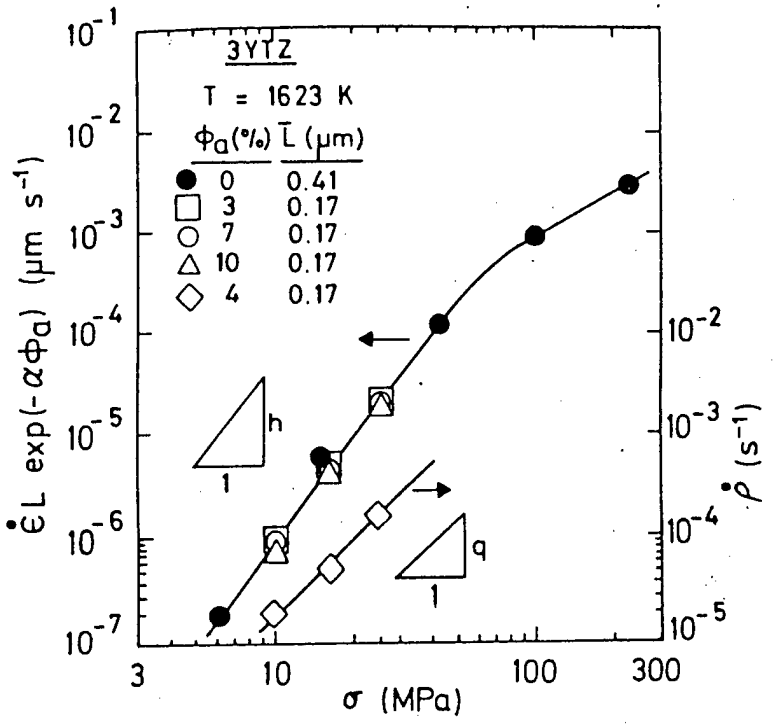

Fig. 2 Variation with stress in creep rate (left) and densification rate (right) [11].

porosity by plotting $\dot{\varepsilon}\exp(-\alpha\phi)$ vs σ. In a manner similar to eqn. 1, the stress dependence of densification rate can be expressed as $\dot{\rho} \propto \sigma^{q}$, where q is a constant. There are two important points to note from these results: (i) creep occurs by an identical mechanism in porous and fully dense 3YTZ, and (ii) the stress exponent for creep deformation and densification are not identical. Thus, while the stress dependence of creep is given as n~3, the stress dependence of the densification rate is expressed as q~2. For plasticity controlled processes, the rate of void growth or void removal $\dot{V} \propto \sigma^{n}$, whereas for a quasi-equilibrium diffusion controlled mechanism $\dot{V} \propto \sigma$. Clearly, the experimental observation of the stress dependence of densification (q=2) rule out the standard models of plasticity control and diffusion.

The experimental data yielded an activation energy of ~600 kJ mol^{-1} for sintering, with or without an applied stress, and creep during densification.

IV. GRAIN GROWTH

Grain growth is also a thermally activated process, and the kinetics of grain growth are expresses usually in the form: $d^{N}-d_0^{N} = Kt$, where N is a constant, K is a constant incorporating the temperature dependence of grain growth, d_0 is the initial grain size and d is the grain size after time t. The constant K may be written as $K=K_0\exp(-Q/RT)$, where Q is the activation energy for grain growth. Nieh and

Wadsworth [10] analyzed grain growth in 3YTZ during static annealing and after superplastic deformation. Superplastic deformation leads to an enhancement in grain growth, and this process is referred to as dynamic grain growth. The study by Nieh and Wadsworth [10] reported activation energies of ~580 and 520 kJ mol^{-1} for static and dynamic grain growth, respectively, assuming N=3. The enhancement in grain growth during superplastic deformation was attributed to a decrease in the activation energy, although the reported differences in activation energies are within the usual range of errors associated with such measurements. An increase in the constant K_0 is an alternative means of rationalizing dynamic grain growth, when the activation energies for static and dynamic grain growth are similar. Other studies on grain growth in superplastic zirconias also indicate activation energies in the range of ~500 to 600 kJ mol^{-1}. In addition, the rate of static grain growth is higher in materials with a higher impurity content.

V. CAVITATION FRACTURE

It is now reasonably well established that failure in many superplastic zirconias occurs by the nucleation, growth and interlinkage of voids in a direction perpendicular to the tensile axis [2,3]. Microstructural inspection revealed that the cavities nucleate predominantly at triple points in a superplastic 3YTZ [11]. In contrast to metallic alloys, there is not much detailed information available on the growth of individual voids, although there is now considerable information available on the evolution of the total level of cavitation. In addition, models have also been developed for the growth of large voids which intersect multiple grain boundaries [9]. Both the presence of a glassy phase and the grain size have a significant effect on ductility [3,12]

VI. DISCUSSION

A common theme underlying all the topics discussed in the present paper is transport of matter from sources to sinks. It is clear that, within the normal errors associated with such measurements, activation energies in the range of ~500 to 600 kJ mol^{-1} are obtained for creep deformation, densification and grain growth. Although creep and grain growth involve vacancy creation, diffusion and annihilation, densification does not require vacancy creation; consequently, it is possible to rule out vacancy creation as a rate controlling step. In addition, as noted in Section 3, since the stress dependence of densification or creep is not unity, it is not possible to attribute these processes to diffusion control. Based on these observations, it is suggested that the annihilation of vacancies at appropriate sinks is the rate controlling mechanism in creep deformation, densification as well as grain growth. Such interface reaction controlled processes inevitably lead to stress exponents greater than one, and there are models available which predict stress exponents of 2 for both creep and densification [9].

VII. SUMMARY AND CONCLUSIONS

(a) There is a transition in stress exponents for creep from a value of ~2 to

~3 with a decrease in stress; the transition stress decreases with an increase in the impurity content and an increase in the grain size of the material.

(b) Porous and fully dense 3YTZ deform by the same mechanism, both involving a stress exponent of ~3. Based on the stress exponent of densification (~2), it is concluded that densification cannot be attributed solely to a diffusion or plasticity controlled mechanism.

(c) The similar values of the activation energy for creep, densification and grain growth suggest strongly that all of these processes are controlled by an interface reaction mechanism involving the annihilation of vacancies at sinks.

ACKNOWLEDGMENTS

This work was supported by DST and USAFOSR.

REFERENCES

[1] Wakai F., Sakaguchi S, Matsuno Y. Superplasticity of yttria-stabilized tetragonal ZrO_2 polycrystals. *Adv. Ceram. Mater.*, 1986, 1: 259-263.

[2] Chokshi AH, Mukherjee AK, Langdon TG. Superplasticity in advanced materials. *Mater. Sci. Eng.*, 1993, R10: 238-274.

[3] Chokshi AH. Superplasticity in fine-grained ceramics: current understanding and future prospects. *Mater. Sci. Eng.*, 1993, A116: 119-33.

[4] Nieh TG, Wadsworth J, Wakai F. Recent advances in superplastic ceramics and ceramic composites. *Inter. Mater. Rev.*, 1991, 36: 146-161.

[5] Carry C. High ductilities, superplastic behaviors and associated mechanisms in fine grained ceramics, in *Superplasticity* (eds. M. Kobayashi and F. Wakai). Materials Research Society, Pittsburgh, PA, 1989: 199-215.

[6] Owen DM, Chokshi AH. Observations of transitions in creep behavior of a superplastic yttria-stabilized zirconia, in *Science and Technology of Zirconia V.* Technomic Publishing Co., Lancaster, PA, 1993: 432-439.

[7] Owen DM, Chokshi AH, to be published.

[8] Hines JA, Chokshi AH. Deformation behavior of a superplastic 2 mol% yttria stabilized zirconia in tension and compression. *Mater. Sci. Forum*, 1994, 170-172: 421-426.

[9] Owen DM, Chokshi AH. Final stage free sintering and sinter forging behavior of a yttria stabilized zirconia, submitted for publication.

[10] Nieh T-G, Wadsworth J. Dynamic grain growth during superplastic deformation of yttria-stabilized tetragonal zirconia polycrystals. *J. Am. Ceram. Soc.*, 1989, 72: 1469-72.

[11] Schissler DJ, Chokshi AH, Nieh T-G, Wadsworth J. Microstructural aspects of superplastic deformation and cavitation failure in a fine grained yttria stabilized tetragonal zirconia. *Acta Metall. Mater.* 1991, 39: 3227-36.

[12] Kajihara K, Yoshizawa Y, Sakuma T. The enhancement of superplastic flow in zirconia polycrystals with SiO2 doping. *ibid.* 1995, 43: 1235-42.

Materials Science Forum Vols. 243-245 (1997) pp. 369-374

Appendix A2

HIGH TEMPERATURE DEFORMATION AND DENSIFICATION IN ALUMINA-YTTRIA COMPOSITES

Saki Krishnamurthy and Atul H. Chokshi
Department of Metallurgy
Indian Institute of Science
Bangalore 560 012
India

Keywords: alumina, yttria, creep, sinter-forging, grain growth

Abstract Pinning by second phase particles offers a potent means for limiting grain growth and enhancing superplasticity in alumina-based ceramics. In the present study, a colloidal technique was used to produce green bodies of alumina-yttria composites; at elevated temperatures, the yttria particles react with alumina to produce YAG particles. The densification and high temperature deformation characteristics of alumina-YAG composites were studied using conventional free sintering and sinter-forging, which involves the application of a compressive stress without any lateral constraints. It is shown that the YAG particles retard both densification and grain growth. The experiments indicate also that the presence of YAG particles does not significantly alter the stress exponent for creep deformation.

Introduction The ability of some fine-grained crystalline materials to deform extensively under tensile loads, termed superplasticity, has been demonstrated now in a wide rang of metallic, intermetallic, ceramic and composite materials [1]. In addition to a fine grain size, superplasticity requires a high strain rate sensitivity, m, where $m = \delta \log \dot{\varepsilon} / \delta \log \sigma$ and $\dot{\varepsilon}$ and σ are the strain rate and stress, respectively. In conventional creep tests, the data are presented as $\dot{\varepsilon} \propto \sigma^n$, where n is termed the stress exponent. Superplasticity is generally associated with $m>0.3$ or $n<3$.

There have been numerous creep studies on polycrystalline alumina revealing $n<3$ [2,3]. However, experiments in tension indicate that alumina exhibits very limited ductility, with elongation to failure of <100% [4]. The low ductility has been attributed partly to deformation enhanced grain growth and cavitation in these materials [5]. Yoshizawa and Sakuma [5] have shown that ductility in alumina can be enhanced by doping with 0.1 wt % MgO, which limits grain growth during high temperature testing. Additions of 20 wt% zirconia also restrict grain growth and facilitate large elongations to failure [6,7]. Carry *et al.* [8,9] have examined deformation in alumina co-doped with 500 ppm each of MgO and Y_2O_3: the dopants led to a finer grain size.

Fully dense structural ceramics are usually processed from powders, and inhomogeneous packing and agglomerates can lead to differential shrinkage during sintering [10] or to favorable sites for cavitation during subsequent mechanical testing [11]. Colloidal processing techniques can be utilized to preclude large agglomerates and to produce favorable packing characteristics in green bodies. Fully dense bodies can then be obtained by sintering the green bodies at elevated temperatures without a load (free sintering) or with a compressive load. Sinter-forging is a technique of applying a compressive load to a specimen without any lateral constraints [12,13]: during sinter-forging, the specimen changes shape due to both densification and creep. Following Raj [14], it is

possible to separate out the densification and plastic creep strains by measuring both the axial strain and either the transverse strain or the density.

The present investigation was undertaken to examine the influence of a large volume fraction of yttria on densification, grain growth and creep in alumina, in order to evaluate the potential for superplasticity in alumina-yttria composites. Based on the phase diagram, it is anticipated that yttria will react with alumina to form the yttrium aluminum garnet (YAG) phase, so that the final product will be an alumina-YAG composite.

Experimental High purity alumina and yttria powders were obtained from Japan from the Taimei Chemicals Corporation and Tosoh, respectively. Two different compositions were chosen for this study: high purity alumina, and alumina-6.24 wt% yttria. The powders were suspended in high purity water to produce a slurry containing ~20 vol% solids. The slurry was dispersed using hydrochloric acid to adjust the pH to ~2, and stirred ultrasonically to break up large agglomerates. For the pure alumina, the dispersed slurry was flocced by adjusting the pH to ~8 using ammonia solution. For the two-phase composition, the individual powders were first dispersed separately, mixed, and then flocced to limit mass segregation by adjusting the pH to ~8 using ammonia solution.

Green bodies of the necessary compositions were prepared by pressure filtering the appropriate slurries at 36 MPa using an Instron machine with a feedback loop to maintain a constant stress. The consolidation was completed typically in ~25 minutes, after which the load was released, the specimen extracted from the die and allowed to air dry for ~12 hours at room temperature. The densities of the green bodies were determined from measurements of the mass and specimen dimensions.

Free sintering was carried out in air at 1673 K using a furnace with superkanthal filaments. The specimens were initially heated rapidly to 1023 K, and then heated to 1673 in one hour at a constant heating rate. The radial shrinkage in the specimen was recorded using alumina dilatometry; the data were recorded continuously using a pc-based data acquisition system. The density vs time profile was displayed continuously, and sintering was terminated when the density did not change appreciably over a few hours.

Sinter-forging experiments were carried out on the cylindrical green bodies at 1673 K under constant load conditions, with initial stresses of 10, 25 and 60 MPa at 1673 K. The green bodies were placed in the furnace and heated to 1673 K using the heating cycle described above for free sintering; the appropriate compressive load was applied immediately upon reaching the testing temperature. The creep (ε_c) and densification (ε_d) strains were determined from measurements of the axial strain and density, as suggested by Raj [14].

The densities of sintered and sinter-forged specimens were obtained using Archimedes' principle with water as the immersion medium. X-ray diffraction was carried out on the composite to examine phase changes that occurred during sintering. Selected specimens were sectioned, polished and examined by scanning electron microscopy to evaluate microstructural changes accompanying densification.

Results and Discussion Specimens heated to the isothermal temperature of 1673 K were cooled immediately upon reaching 1673 K to examine the possibility of phase changes during the constant heating rate cycle from 1023 to 1673 K. Analysis of the X-ray diffraction patterns of the composite revealed only two phases: alumina and Yttria Aluminum Garnet (YAG); the yttria had reacted completely to form YAG. Based on the phase diagram and crystal structure, the 6.24wt% yttria containing alumina corresponds to a composite of alumina - 10 vol% YAG. The true density of alumina and the 10vol% YAG containing composite are 3.96 and 4.01 g cm^{-3}, respectively.

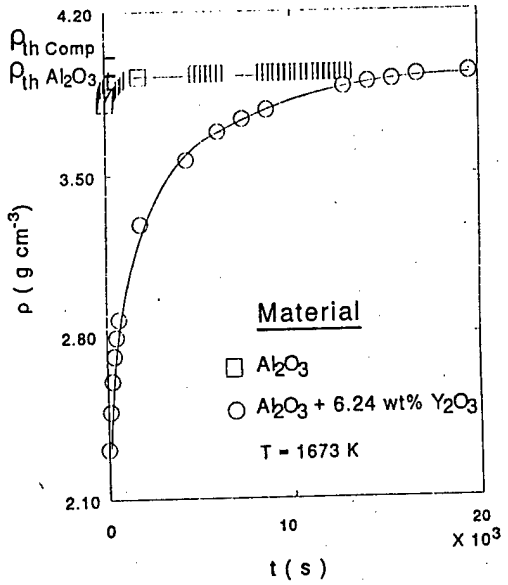

Fig. 1 Variation in density with time for high purity alumina and the composite during free sintering.

Free Sintering: The green densities of the pressure filtered specimens of alumina and alumina-6.24 wt% yttria were 2.1 and 1.9 g cm^{-3}, respectively, which correspond to relative densities of 53 and 47 %. Figure 1 illustrates the variation in density with time for the alumina and the composite. Inspection reveals that near full density is obtained in pure alumina within ~30 minutes, whereas the composite exhibits a relative density of only ~98 % even after sintering for 6 hours. Clearly, the presence of the YAG phase has retarded sintering significantly in the composite. The presence of a second phase will increase the effective path length for diffusion, and this can lead to a decrease in the densification rate.

An early study by Delauney *et al.* [15] indicated that minor additions of yttria (<1%) were beneficial to the sintering of alumina. A more recent study by Chae *et al.* [16] concluded that the optimum level of yttria for enhancing densification in an alumina- titanium carbide composite was 0.35 wt%; further increases in yttria content led to a decrease in the densification rate. Carry *et al.* [8,9] have examined the segregation of yttrium to grain boundaries and the subsequent formation of YAG in grain boundaries with either an increase in the grain size or an increase in the level of yttria content.

Sinter-Forging: Figures 2 and 3 depict the variation with time in the density and the creep strain for pure alumina and the composite, respectively. For pure alumina, the initial density at the sinter-forging temperature was very high, and the amount of creep strain accumulated is relatively small (~4%). In contrast, significant creep strains on the order of ~21% were obtained during sinter-forging in the composite.

Due to the relative high initial densities in alumina, it was not possible to extract a meaningful stres exponent for creep. However, the data for the composite could be used to calculate

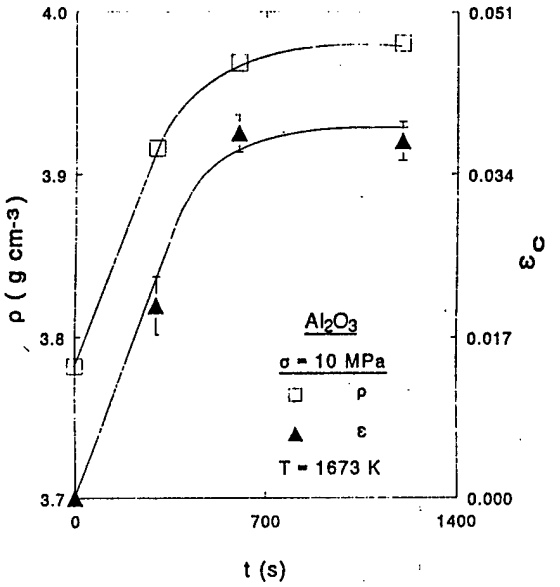

Fig. 2 Variation in density and creep strain with time for pure alumina sinter-forged at 10 MPa.

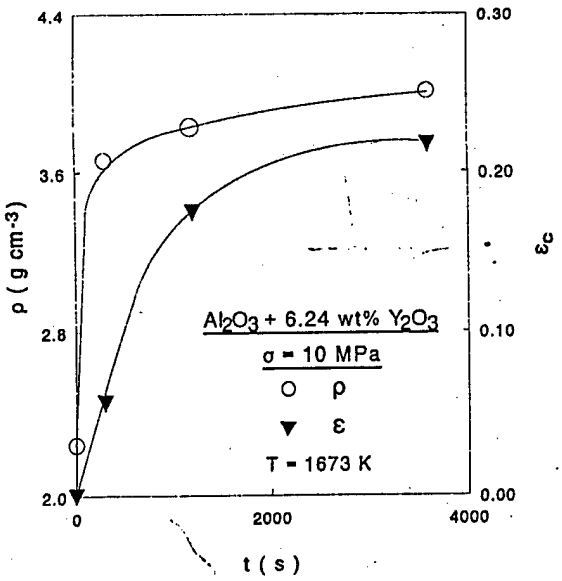

Fig. 3 Variation in the density and creep strain for the alumina-YAG composite sinter-forged at 10 MPa.

9. P.Gruffel and C. Carry, J. Euro. Ceram. Soc., 11 189 (1993).
10. F.F. Lange, J. Am. Ceram. Soc., 72 3 (1989).
11. A.H. Chokshi, Superplasticity in Advanced Materials : edited by S. Hori, M. Tokizane and N. Furushiro, pp171 .
12. M.N. Rahaman, L.C. DeJonghe and R.J. Brook, J. Am. Ceram. Soc., 69 58 (1986).
13. K.R. Venkatachari and R. Raj, J. Am. Ceram. Soc., 69 135 (1986).
14. R. Raj, J. Am. Ceram. Soc., 65 C46 (1982).
15. D. Delauney, A.N. Huntz and P. Lacombe, J. of Less Common Metals, 70 115 (1980).
16. K.W. Chae, D.Y. Kim, B.C. Kim and K.B. Kim, J. Am. Ceram. Soc., 76 C185 (1993).
17. G.S. Corman, J. Mater. Sci., 12 [6] 379 (1993).
18. T.A. Parthasarathy, T.I. Mah, and K. Keller, J. Am. Ceram. Soc., 75 [7] 1756 (1992).
19. T.A. Parthasarathy, T.I. Mah and L.E. Matson, J. Am. Ceram. Soc., 76 [1] 29 (1992).
20. W.J. Kim, J. Wolfenstine and O.D. Sherby, Acta Metall. Mater., 39 [2] 199 (1991).
21. A.H. Chokshi, Mater. Sci. Forum, *in press* (1996).
22. T. Sakuma, this proceedings (1997).

journal

Appendix A3

J. Am. Ceram. Soc., 82 [10] 2613–18 (1999)

Dense Amorphous Zirconia–Alumina by Low-Temperature Consolidation of Spray-Pyrolyzed Powders

Ashutosh S. Gandhi, Vikram Jayaram,* and Atul H. Chokshi*

Department of Metallurgy, Indian Institute of Science, Bangalore 560 012, India

Metastable amorphous ZrO_2–Al_2O_3 powders were hot-pressed at low temperatures (873 and 923 K), under moderately high pressures (500 and 750 MPa), and amorphous pellets with 1%–8% porosity were obtained. Crystallization of the amorphous pieces in the temperature range of 1173–1673 K produced a range of ultrafine microstructures, the finest of which had grains of tetragonal (ZrO_2–40-mol%-Al_2O_3) solid solution 6–8 nm in size that formed at 1173 K. Submicrometer grain sizes of the equilibrium monoclinic ZrO_2 and α-Al_2O_3 were stable against coarsening at 1673 K. The new technique was applied to produce a SiC-reinforced composite with an amorphous ZrO_2–80-mol%-Al_2O_3 matrix; the high matrix sinterability overcame the reinforcement constraint. The results suggest a possible solution to the difficulties in the bulk processing of amorphous, nanocrystalline, and other novel ceramics.

I. Introduction

METASTABLE ceramics that are produced using nonequilibrium processing techniques such as rapid solidification[1,2] and chemical precursor synthesis[3] have been known to possess interesting and potentially useful properties, such as hard or soft magnetic characteristics, semiconductivity, varistor action, and optical transmittivity. In addition to possessing attractive properties, a metastable phase may serve as a precursor to a desired microstructure; for instance, controlled crystallization of an amorphous phase is a route to produce a nanocrystalline structure.[4] Nanocrystalline ceramics are being widely studied because of their potential for novel functional and mechanical properties.[4–6] Among the various attractive properties, the possibility of superplasticity at high strain rates and/or low temperatures has spurred many research activities in regard to the processing of nanocrystalline ceramics.

To study and use the nanostructured and other metastable ceramics extensively, it is important to synthesize these materials in bulk, dense form with control of the fine scale of the structure. Such efforts have not been entirely successful. Consolidation of particulate nanocrystalline and other metastable ceramics into dense forms requires activation in the form of high temperature, static or dynamic loading, or a combination of these conditions. Such activation also triggers transformation to a more stable phase and grain growth,[7–20] which leads to the loss of the initial desired structure by the time full density is attained. On the other hand, conditions that allow the desired metastable phase or nanometric grain size to be retained may not be adequate for complete densification. In the present study, the understanding of metastable phase synthesis and characteristics[3,21–26] was applied to the hot pressing of amorphous ZrO_2–Al_2O_3 powders that have been produced via spray pyrolysis to identify a pressure–temperature window in which consolidation would be possible without losing the metastable amorphous phase.

(1) *Metastability in Spray-Pyrolyzed ZrO_2–Al_2O_3*

Spray pyrolysis is a route to the synthesis of amorphous and other metastable phases in ceramics at relatively low temperatures (≤1100 K).[3,27] Because of such low synthesis temperatures, the equilibrium state can be suppressed kinetically and the system may evolve through many metastable states.[22]

Studies on metastable microstructures in the ZrO_2–Al_2O_3 powders produced via the spray pyrolysis of aqueous zirconium acetate and aluminum nitrate solutions[23,24] established that the product of spray pyrolysis was amorphous for all compositions. On the ZrO_2-rich end, up to 40 mol% Al_2O_3, a single-phase nanocrystalline tetragonal (t) $ZrO_2(Al_2O_3)$ solid solution crystallized when the amorphous powder was heated. With 40 mol% Al_2O_3, the phase evolution with temperature (K) was as follows:

$$\text{Amorphous} \xrightarrow{\sim 1143\text{K}} t\text{-}ZrO_2(Al_2O_3) \xrightarrow{\sim 1273\text{K}}$$

$$t\text{-}ZrO_2 + \gamma\text{-}Al_2O_3 \xrightarrow{\sim 1673\text{K}} m\text{-}ZrO_2 + \alpha\text{-}Al_2O_3$$

where m denotes monoclinic. The grain sizes remained <100 nm after holding at 1273 K for up to 100 h, which indicates the stability of the ultrafine microstructure.[24]

(2) *Background to Hot Pressing of Amorphous ZrO_2–Al_2O_3*

In previous hot-pressing experiments[25,26] on spray-pyrolyzed amorphous ZrO_2–40 mol% Al_2O_3 under 1 GPa hydrostatic pressure, the high pressure accelerated the formation of crystalline phases that were more dense and closer to equilibrium. Thus, a sample pressed at 973 K was already crystalline, partitioned to some extent, and almost fully dense. In contrast, another sample that was pressed at 1173 K consisted of the equilibrium m-ZrO_2 and α-Al_2O_3 phases and was significantly porous. These results imply that the further the phases are from equilibrium, the better the densification, despite the substantially lower temperature. Also, the theory of nucleation, applied to the transformation of a parent phase (crystalline or amorphous) into a denser phase, predicts that pressure is less effective in accelerating nucleation at lower temperatures.[26]

In the present study, hot-pressing experiments were performed at comparatively lower temperatures (873 and 923 K) and pressures (500 and 750 MPa) in an attempt to prevent crystallization of the amorphous phase and yet provide enough activation to the densification process in the amorphous powder compact. As described later in this paper, our attempts were successful in producing dense amorphous compacts of ZrO_2–Al_2O_3 with up to 99% relative density. The dense amorphous compacts were heat-treated to produce nanocrystalline micro-

A. Jagota—contributing editor

Manuscript No. 190354. Received February 24, 1998; approved January 28, 1999.
Supported by the Dept. of Science and Technology (India), the Asian Office of Aerospace Research and Development (Tokyo, Japan) through the U.S. Air Force Office of Scientific Research (AFOSR), and the Dept. of Atomic Energy (India) through the Dr. K. S. Krishnan Fellowship to author ASG.
Based on a poster presented at Ceramics Processing '97, Santa Barbara, CA, Sept. 1997.
*Member, American Ceramic Society.

structures, which demonstrates the feasibility of producing bulk nanocrystalline ceramics through this route.

The new processing route, which involved the hot pressing of a metastable amorphous phase, was used to overcome the well-known problem of constrained sintering in ceramic composite processing.[28–31] The presence of nonsintering reinforcement particles retards the sintering rate of a conventional powder compact. In the present case, the constraint of the SiC reinforcement was overcome by the enhanced densification of the amorphous ZrO_2–Al_2O_3 phase during hot pressing. The low densification temperature (923 K) eliminates the need for vacuum or an inert atmosphere, as far as the oxidation of SiC is concerned. A strong and refractory equilibrium matrix microstructure can be produced by heat treating after densification.

II. Experimental Procedure

(1) Production and Characterization of Amorphous Powders

Amorphous powders of composition ZrO_2–40 mol% Al_2O_3 (hereafter denoted as Z40A) and ZrO_2–80 mol% Al_2O_3 (hereafter denoted as Z80A) were obtained by spraying aqueous solutions that contained both zirconium nitrate and aluminum nitrate onto a Teflon-coated pan that was maintained at a temperature of 523 ± 10 K. A composite powder (ZASC), with 7.7 wt% SiC particles (SiC_p) dispersed in amorphous ZrO_2–80 mol% Al_2O_3, was produced by adding SiC particles <3 μm in size to the spraying solution. Thermogravimetric analysis (TGA) (Model TG-171, Cahn Instruments, Cerritos, CA) was performed on the as-sprayed Z40A and Z80A powders, with a heating rate of 10 K/min. The temperature ranges of crystallization were identified by introducing as-sprayed powder into a furnace that already had been heated to the desired temperature and removing it after a certain duration (up-quenching). X-ray diffractometry (XRD) (Model JDX-8030, JEOL, Tokyo, Japan) was used to identify the phases that were present. Differential thermal analysis (DTA) (Polymer Laboratories, Epsom, Surrey, U.K.), at a heating rate of 10 K/min, was performed on as-sprayed Z40A powder to confirm the crystallization temperature.

The true densities of the amorphous phases that were obtained via pyrolysis of the as-sprayed Z40A powder by heating to temperatures of 1023 and 1073 K were measured via pycnometry, using 25 mL specific-gravity bottles and deionized water.[32] Weights of the bottles with powders and water were measured after allowing the water to fill all the interparticle spaces by keeping the bottles under vacuum for 5 and 15 d for the powders that were obtained at 1023 and 1073 K, respectively. The effect of closed porosity was minimized by grinding the powders in an agate mortar and pestle.

(2) Hot Pressing

The starting powders and the conditions that were used for the consolidation experiments are listed in Table I. Hot pressing was performed on the as-sprayed agglomerated powders, as well as those without agglomerates. To produce deagglomerated powders, the as-sprayed powders first were decomposed by holding at 1073 K for 1 h, so that all the volatile matter, except that retained up to a temperature of 1450 K (see next section), was driven out. Agglomerates larger than ~10 μm were removed via sedimentation for 5 min in a deionized-water column 15 cm tall, based on a true density of 3.3 g/cm³ from pycnometry for Z40A. A settling time of 5.5 min was used to sediment the ZASC, which resulted in a finer powder.

A nickel-based superalloy die with an internal diameter of 5 mm was used for consolidation in a screw-driven universal testing machine (Instron, Canton, MA) that was fitted with a furnace. BN powder was used for lubrication and flexible graphite foils 0.2 mm thick were used as spacers between the pellet and the punches. Cold compaction was conducted at 750 MPa.

Prior to hot pressing, the green compacts of the as-sprayed Z40A powder were heated to 1023 K for 5 min, to cause decomposition of the as-sprayed material and concurrent sintering. As reported previously,[32] this step leads to higher starting densities prior to hot pressing than does compaction of the decomposed powders. The compacts at this stage had relative densities of ~70%–75%. After cooling to 873 or 923 K, a pressure of 500 or 750 MPa was applied for up to 90 min. The deagglomerated powders were heated directly to 923 K and pressed at 750 MPa. In all the experiments, the heating and cooling rates were 20–30 K/min. The pressure was released before cooling to room temperature.

Porosity measurements, using quantitative optical microscopy and Vickers hardness measurements (Model HMV-2000, Shimadzu Co., Kyoto, Japan), were made on the polished hot-pressed pellets.

(3) Crystallization of Hot-Pressed Pellets

DTA was performed on a hot-pressed pellet from agglomerated powder, to compare its crystallization behavior with the loose powder. Some of the hot-pressed samples were sectioned and the small pieces were subjected to crystallization by up-quenching for temperatures <1273 K and by slow heating for higher temperatures up to 1673 K. Powder XRD patterns were taken from the heat-treated pieces (Guinier Type 642, Huber, Chiemsee, Germany). Scanning electron microscopy (SEM) (Model JSM-840A, JEOL) was performed on samples that were heat-treated to 1673 K after coating with carbon or gold. Image analysis was performed on the SEM micrographs from gold-coated samples to measure the porosity that was introduced during crystallization.

III. Results and Discussion

(1) Powder Characteristics

The as-sprayed powders are highly agglomerated, with a primary particle size of <10 μm. TGA of as-sprayed Z40A (Fig. 1) shows that the sample loses ~25% of its weight by 520 K, which is due to the moisture that has been absorbed during storage. Between 820 and 1020 K, an additional weight loss of 2.7% occurs. The weight remains constant between 1020 and 1450 K, with a final weight loss of 0.6% that occurs at ~1470

Table I. Details of the Hot Pressing of Amorphous Spray-Pyrolyzed ZrO_2–Al_2O_3

Composition	Starting condition	Temperature (K)	Pressure (MPa)	Time (min)	Porosity† (%)	Hardness (GPa)
Z40A	As-sprayed	923	750	5	4	3.2
Z40A	As-sprayed	923	750	30	4	3.4
Z40A	As-sprayed	923	750	60	8	
Z40A	As-sprayed	923	750	90	2	4.2
Z40A	As-sprayed	923	500	60	4	2.8
Z40A	As-sprayed	873	750	60	4	
Z40A	Deagglomerated	923	750	60	4	1.6
ZASC	Deagglomerated	923	750	60	1	

†Except for the deagglomerated samples, porosity was measured in the dense regions of the samples, i.e., excluding voids larger than ~50 μm.

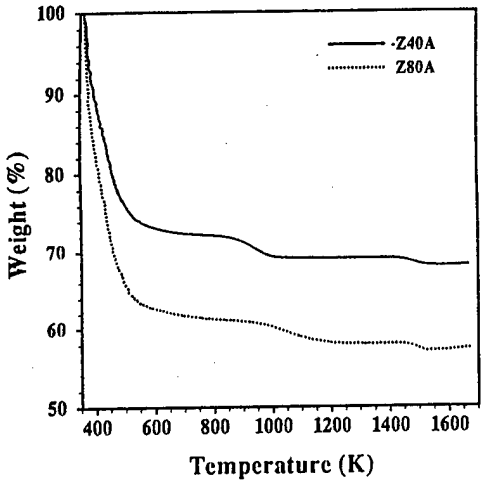

Fig. 1. TGA plots for as-sprayed ZrO_2–Al_2O_3 powders. The weight remains constant over the temperature range of 1020–1450 K for Z40A and 1170–1450 K for Z80A, and the phase evolution of the amorphous phases occurs in these temperature ranges of constant weight.

K. Figure 1 also shows that the Z80A powder loses more moisture, up to 520 K. The second weight loss of 2.7% occurs over a larger temperature range, 920–1170 K, whereas 0.9% of the weight is lost at ~1470 K.

The XRD patterns in Fig. 2 show that the Z40A powder is amorphous after 5 min at 1133 K. The beginning of crystallization to t-ZrO_2 is noted after 5 min at 1153 K, whereas well-developed peaks appear at 1193 K. This temperature range corresponds to the sharp exotherm at 1188 K in the DTA curve (Fig. 3). The α-Al_2O_3 and m-ZrO_2 phases appear at 1473 K, although t-ZrO_2 is still the major phase. After heat treatments at 1573 and 1673 K, the predominant phases are m-ZrO_2 and α-Al_2O_3, with some retained t-ZrO_2. The sequence of phase evolution is the same as that reported previously,[23,24] although the temperatures at which the various phases appear are different.

The Z80A composition begins to crystallize at ~1173 K, with the appearance of t-ZrO_2 peaks; γ-Al_2O_3 peaks appear at 1273 K, whereas the equilibrium phases form at higher temperatures. The behavior of this Al_2O_3-rich composition is similar to the ZrO_2-rich end, because the amorphous phase is retained up to high enough temperatures to enable hot-pressing experiments to be performed.

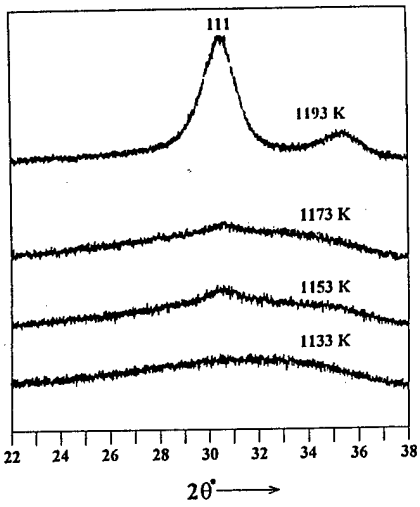

Fig. 2. XRD patterns of Z40A powder heat-treated at the indicated temperatures; the onset of crystallization is indicated by the appearance of the 111 peak of tetragonal $ZrO_2(Al_2O_3)$.

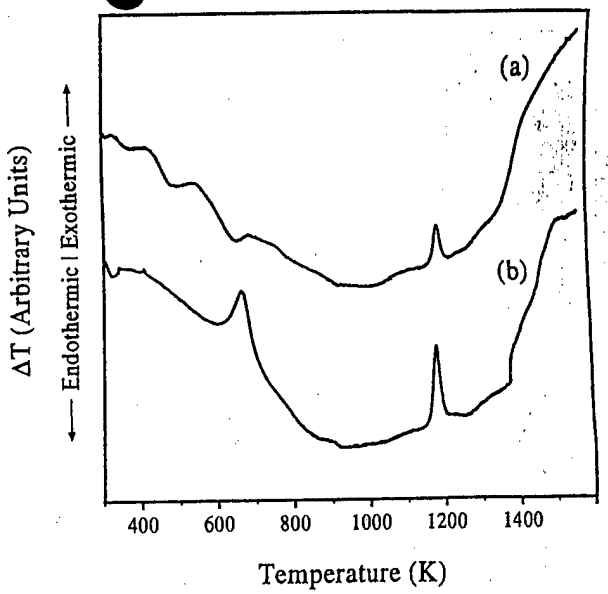

Fig. 3. DTA plots from (a) the as-sprayed Z40A powder and (b) a pellet hot-pressed at 873 K. The exotherms at 1173 K from both materials coincide with the appearance of a diffraction peak corresponding to the {111} planes from a tetragonal $ZrO_2(Al_2O_3)$ solid solution.

(2) *Hot Pressing of Amorphous ZrO_2–40 mol% Al_2O_3*

Table I summarizes the results of the hot-pressing experiments. The XRD pattern in Fig. 4 from the Z40A pellet hot-pressed for the longest duration among these experiments (90 min) shows that it is amorphous. This result is corroborated by DTA that was conducted on a sample that was hot-pressed at 873 K (Fig. 3), which reveals the same exotherm at 1173 K as observed in the case of the powder. Optical micrographs of the hot-pressed pellets from as-sprayed Z40A (Fig. 5) show that significant densification occurs within 5 min of pressing at 923 K and 750 MPa. Because the as-sprayed powder is highly agglomerated, the hot-pressed pellets in Fig. 5 have large voids (>50 μm) that surround the regions of very low porosity. Po-

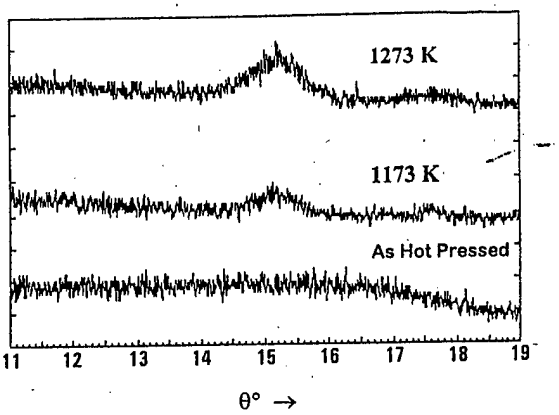

Fig. 4. X-ray diffractograms of hot-pressed Z40A samples. All the samples remain amorphous after hot pressing, and the amorphous phase crystallizes after heat treatment at >1173 K to a tetragonal $ZrO_2(Al_2O_3)$ solid solution with grains 6–8 nm in size.

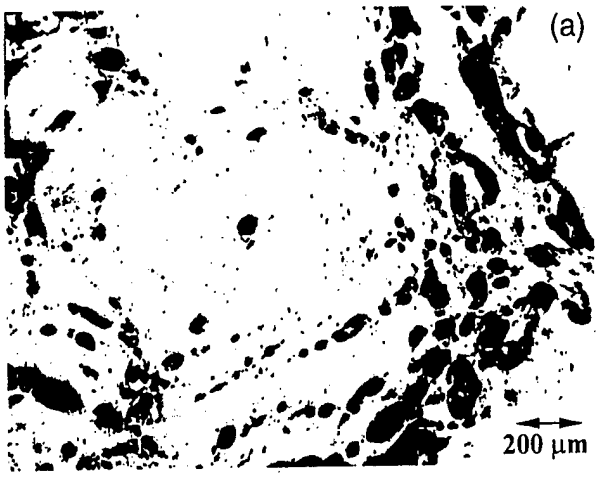

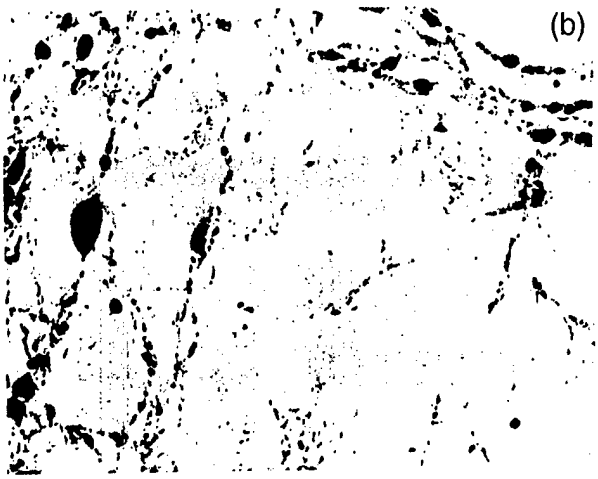

Fig. 5. Optical micrographs of amorphous Z40A hot-pressed at 923 K and 750 MPa for (a) 5 and (b) 90 min. Regions of low porosity form via densification of the agglomerates; the large pores originate from voids between agglomerates.

rosity in these dense regions has been measured via optical image analysis and is listed in Table I. No correlation is apparent between the time of hot pressing and the final porosity, although the porosity after 90 min is the lowest in this set of experiments. Also, neither a less-severe pressure of 500 MPa nor a lower temperature of 873 K seems to affect the densification process significantly. The large voids due to agglomeration may have masked the role of the hot-pressing parameters. However, these results also indicate the possibility that significant densification can occur at lower temperatures and pressures or in a short duration of a few minutes.

Hot pressing of the decomposed, deagglomerated powder yields a uniform distribution of fine porosity (Fig. 6), which is measured to be 4%, including a few large pores (~50 μm). The porosity distribution is fairly uniform throughout the pellet. The overall porosity is sensitive to deagglomeration; therefore, complete pore elimination should be possible by using finer amorphous powders (particles <1 μm in size), which can be accomplished, in principle, by comminution or by improving the spray-pyrolysis technique.

The Vickers hardness with a 500 g load was measured on the Z40A samples, and the values are listed in Table I. The measured hardness of the sample from deagglomerated powder is much lower than those from the as-sprayed (agglomerated) powders. Because of the uniform pore distribution in the sample from the deagglomerated powder, more pores affect the

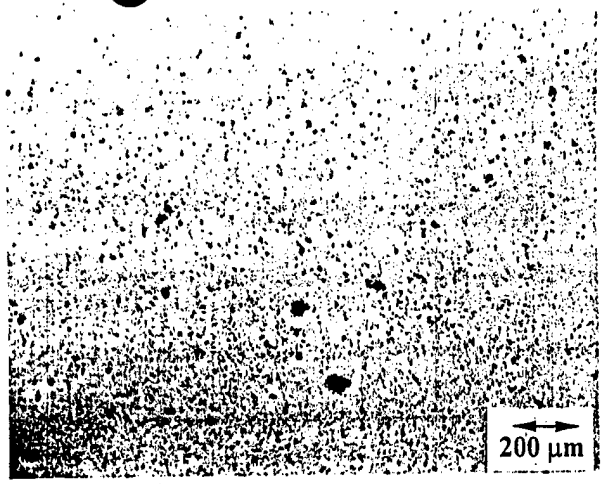

Fig. 6. Uniform pore distribution in a hot-pressed amorphous Z40A sample; the uniformity is due to the removal of agglomerates larger than ~10 μm. This result indicates that hot pressing finer amorphous powders (particles <1 μm in size) may eliminate all the porosity.

indentation, compared to the pellets from agglomerated powder for which the measurements are made on regions almost free of pores. Hence, the hardness measured on the sample pressed for 90 min, which has the lowest measured porosity, is taken as the hardness of the amorphous phase. It is lower by a factor of ~2.5 than the typical hardness value for partially stabilized ZrO_2 (~10 GPa) and by a factor of ~4.5 than that for α-Al_2O_3 (~18 GPa).

(3) Crystallization of Amorphous ZrO_2–40-mol%-Al_2O_3 Pellets

Crystallization of the amorphous hot-pressed pellets at 1173–1273 K, similar to that of the free, as-sprayed powder, produces a t-$ZrO_2(Al_2O_3)$ solid solution (Fig. 4) with grains 6–8 nm in size (measured from the broadening of the 111 peak and by the application of Scherrer's formula, after subtracting instrumental broadening). The exothermic peak shown in curve (b) of Fig. 3 at 1178 K corresponds to crystallization. (A broad peak is observed at 664 K, the reasons for which are not known.) The pellets developed additional porosity after crystallization; for instance, a sample heat-treated at 1673 K for 2 h contained ~31% porosity in regions that would be fully dense in the amorphous state. The size of these voids was a few hundred nanometers. The additional porosity is due to the large contraction that is expected from the molar volume difference between the amorphous and crystalline phases. After decomposition at 1073 K, the density of the amorphous phase, as measured by pycnometry,[32] was 3.3 g/cm^3, which is 34% smaller than the density in the equilibrium state (5 g/cm^3 with m-ZrO_2 and α-Al_2O_3). As described previously in this section, transformation to the α-Al_2O_3 and m-ZrO_2 equilibrium phases began at 1473 K, at which stage the hot-pressed pellet has a ZrO_2 grain size of 100 nm. Table II and Fig. 7 show that the microstructure, which consists of m-ZrO_2, α-Al_2O_3, and some

Table II. Grain Sizes in ZrO_2–40 mol% Al_2O_3 Hot-Pressed in the Amorphous State and Crystallized by Heating as Indicated

Temperature (K)	Time (min)	ZrO_2 grain size (nm)
1273	5	6†
1473	5	100‡
1673	5	230‡
1673	60	290‡

†Measured from XRD peak broadening. ‡Mean intercept, as measured via SEM.

sixfold coordinations. These observations, together with the low hardness of the amorphous material, imply that the amorphous phase has a more open structure, compared to the equilibrium phases, and also is likely to possess high concentrations of point defects, because of nonstoichiometry and nonequilibrium processing conditions. Consequently, it may possess high ionic mobilities and low viscosity. Presently, these observations are unresolved issues. However, the present work is a successful application of the understanding of metastable phase synthesis and behavior to the production of novel ceramic microstructures in bulk form.

IV. Conclusions

(1) Hot-pressing experiments on spray-pyrolyzed amorphous ZrO_2–40 mol% Al_2O_3 (Z40A) powders at 873–923 K and 500–750 MPa have established that the amorphous powders have much-greater sinterability than the equilibrium phases.

(2) Hot pressing of deagglomerated (<10 μm) powder produced a sample with uniformly distributed fine pores and a total porosity of only 4%.

(3) The amorphous Z40A phase has a very low hardness of ~4.2 GPa, compared to the equilibrium phases (>10 GPa for partially stabilized ZrO_2 and 18 GPa for α-Al_2O_3).

(4) Heat treatment of the hot-pressed pellets produced a range of bulk ultrafine microstructures, the finest of which consists of a tetragonal $ZrO_2(Al_2O_3)$ solid solution with grains 6–8 nm in size. The two-phase equilibrium microstructure was stable against rapid coarsening at 1673 K.

(5) Hot pressing of SiC-particle-reinforced amorphous ZrO_2–80 mol% Al_2O_3 produced a composite with only 1% porosity, which demonstrates the potential of this processing route of hot pressing an amorphous phase.

(6) Low true density of the amorphous phase indicates an open structure and high point-defect concentrations, which may lead to high diffusivities and low viscosities, which may be the causes for the high sinterability of the amorphous phases.

Acknowledgment: The authors are grateful to Mr. Kaustubh Kulkarni for assistance in preparing the ZrO_2–80-mol%-Al_2O_3 and SiC_p composite powders.

References

[1]L. A. Jacobson and J. McKittrick, "Rapid Solidification Processing," *Mater. Sci. Eng. R*, **R11**, 355–408 (1994).

[2]M. C. Brockway and R. R. Wills, "Rapid Solidification of Ceramics, a Technology Assessment," Rep. No. MCIC-84-49, Metals and Ceramics Information Center, Columbus, OH, 1984.

[3]C. G. Levi, "Metastability and Microstructure Evolution in the Synthesis of Inorganics from Precursors," *Acta Mater.*, **46**, 787–800 (1998).

[4]C. Suryanarayana, "Nanocrystalline Materials," *Int. Mater. Rev.*, **40**, 41–64 (1995).

[5]H. Gleiter, "Materials with Ultrafine Microstructures: Retrospectives and Perspectives," *Nanostruct. Mater.*, **1**, 1–19 (1992).

[6]R. W. Siegel, "Nanostructured Materials—Mind over Matter," *Nanostruct. Mater.*, **3**, 1–18 (1995).

[7]H. Watanabe, K. Hirota, O. Yamaguchi, S. Inamura, H. Miyamoto, H. Shiokawa, and K. Tsuji, "Hot Isostatic Pressing of Tetragonal ZrO_2 Solid-Solution Powders Prepared from Acetylacetonates in the System ZrO_2–Y_2O_3–Al_2O_3," *J. Mater. Sci.*, **29**, 3719–23 (1994).

[8]M. Fukuya, K. Hirota, O. Yamaguchi, H. Kume, S. Inamura, H. Miyamoto, N. Shiokawa, and R. Shikata, "Sintering and Characterization of Yttria-Stabilized Zirconia with Alumina Derived from Solid Solution," *Mater. Res. Bull.*, **29**, 619–28 (1994).

[9]J. McKittrick, B. Tunaboylu, and J. Katz, "Microwave and Conventional Sintering of Rapidly Solidified Al_2O_3–ZrO_2 Powders," *J. Mater. Sci.*, **29**, 2119–25 (1994).

[10]H. Ito, Y. Yamasaki, K. Takagi, and H. Kuroki, "Effect of Zirconia Content on the Strength of Mullite Ceramics Hot-Pressed from Rapidly Solidified Powders," *J. Jpn. Soc. Powder Powder Met.*, **43**, 1466–72 (1996).

[11]D. Y. Jeng and M. N. Rahaman, "Effect of Rigid Inclusions on the Sintering of Mullite Synthesized by Sol–Gel Processing," *J. Mater. Sci.*, **28**, 4421–26 (1993).

[12]D. Y. Jeng and M. N. Rahaman, "Sintering and Crystallization of Mullite Powder Prepared by Sol–Gel Processing," *J. Mater. Sci.*, **28**, 4904–909 (1993).

[13]T. Hirano, K. Niihara, T. Ohji, and F. Wakai, "Improved Creep Resistance of Si_3N_4 Nanocomposites Fabricated from Amorphous Si-C-N Precursor Powder," *J. Mater. Sci. Lett.*, **15**, 505–507 (1996).

[14]T. Hirano, K. Izaki, and K. Niihara, "Microstructure and Thermal Conductivity of Si_3N_4/SiC Nanocomposites Fabricated from Amorphous Si-C-N Powders," *Nanostruct. Mater.*, **5**, 809–18 (1995).

[15]P. Sajgalik, J. Dusza, F. Hofer, P. Warbichler, M. Reece, G. Boden, and J. Kozankova, "Structural Development and Properties of SiC–Si_3N_4 Nano/Macro-Composites," *J. Mater. Sci. Lett.*, **15**, 72–76 (1996).

[16]D. T. Castro and J. Y. Ying, "Synthesis and Sintering of Nanocrystalline Titanium Nitride," *Nanostruct. Mater.*, **9**, 67–70 (1997).

[17]D.-J. Chen and M. J. Mayo, "Rapid Rate Sintering of Nanocrystalline ZrO_2–3 mol% Y_2O_3," *J. Am. Ceram. Soc.*, **79** [4] 906–12 (1996).

[18]M. J. Mayo, "Processing of Nanocrystalline Ceramics from Ultrafine Particles," *Int. Mater. Rev.*, **41**, 85–115 (1996).

[19]D. M. Owen and A. H. Chokshi, "An Evaluation of the Densification Characteristics of Nanocrystalline Materials," *Nanostruct. Mater.*, **2**, 181–87 (1993).

[20]D. J. Chen and M. J. Mayo, "Densification and Grain Growth of Ultrafine 3 mol% Y_2O_3–ZrO_2 Ceramics," *Nanostruct. Mater.*, **2**, 469–78 (1993).

[21]V. Jayaram, C. G. Levi, T. Whitney, and R. Mehrabian, "Characterization of Al_2O_3–ZrO_2 Powders Produced by Electrohydrodynamic Atomization," *Mater. Sci. Eng. A*, **A124**, 65–81 (1990).

[22]V. Jayaram, M. de Graef, and C. G. Levi, "Metastable Extension of the Fluorite Phase Field in Y_2O_3–ZrO_2 and its Effect on Grain Growth," *Acta Metall. Mater.*, **42**, 1829–46 (1994).

[23]M. L. Balmer, F. F. Lange, and C. G. Levi, "Metastable Phase Selection and Partitioning for $Zr_{(1-x)}Al_xO_{(2-x/2)}$ Materials Synthesized with Liquid Precursors," *J. Am. Ceram. Soc.*, **77** [8] 2069–75 (1994).

[24]M. L. Balmer, F. F. Lange, V. Jayaram, and C. G. Levi, "Development of Nano-Composite Microstructures in ZrO_2–Al_2O_3 via the Solution Precursor Method," *J. Am. Ceram. Soc.*, **78** [6] 1489–94 (1995).

[25]V. Jayaram, R. S. Mishra, B. Majumdar, C. Lesher, and A. K. Mukherjee, "Dense Nanometric ZrO_2–Al_2O_3 from Spray Pyrolysed Powder," *Colloids Surf. A*, **133**, 25–31 (1998).

[26]R. S. Mishra, V. Jayaram, B. Majumdar, C. E. Lesher, and A. K. Mukherjee, "Preparation of a ZrO_2–Al_2O_3 Nanocomposite by High Pressure Sintering of Spray Pyrolysed Powders," *J. Mater. Res.*, **14**, 834–40 (1999).

[27]G. L. Messing, S.-C. Zhang, and G. V. Jayanthi, "Ceramic Powder Synthesis by Spray Pyrolysis," *J. Am. Ceram. Soc.*, **76** [11] 2707–26 (1993).

[28]A. S. Gandhi, A. Saravanan, and V. Jayaram, "Containerless Processing of Ceramics by Aerodynamic Levitation," *Mater. Sci. Eng. A*, **A221**, 68–75 (1996).

[29]A. Jagota, "Simulation of Viscous Sintering of Coated Particles," *J. Am. Ceram. Soc.*, **77** [8] 2237–39 (1994).

[30]C.-L. Fan and M. N. Rahaman, "Factors Controlling the Sintering of Ceramic Particulate Composites: I, Conventional Processing," *J. Am. Ceram. Soc.*, **75** [8] 2056–65 (1992).

[31]R. K. Bordia and G. W. Scherer, "On Constrained Sintering—I. Constitutive Model for a Sintering Body," *Acta Metall.*, **36**, 2393–97 (1988).

[32]A. S. Gandhi, V. Jayaram, and A. H. Chokshi, "Phase Evolution and Densification of Spray-Pyrolysed ZrO_2–Al_2O_3 Powders," *Mater. Sci. Forum*, **243–245**, 227–32 (1997).

[33]A. R. Boccaccini, D. H. Pearce, and P. A. Trusty, "Pressureless Sintering and Characterization of Al_2O_3-Platelet Reinforced Barium-Magnesium Aluminosilicate Glass-Ceramic Composites," *Composites (Guildford, U.K.), A*, **28A**, 505–10 (1997).

[34]A. R. Boccaccini, W. Stumpfe, D. M. R. Taplin, and C. B. Ponton, "Densification and Crystallization of Glass Powder Compacts During Constant Heating Rate Sintering," *Mater. Sci. Eng. A*, **A219**, 26–31 (1996).

[35]M. D. Glendenning and W. E. Lee, "Microstructural Development on Crystallizing Hot-Pressed Pellets of Cordierite Melt-derived Glass Containing B_2O_3 and P_2O_5," *J. Am. Ceram. Soc.*, **79** [3] 705–13 (1996).

[36]M. J. Reece, C. A. Worrell, G. J. Hill, and R. Morrell, "Microstructures and Dielectric Properties of Ferroelectric Glass-Ceramics," *J. Am. Ceram. Soc.*, **79** [1] 17–26 (1996).

[37]I. A. Cornejo, J. Collier, and M. J. Haun, "Ferroelectric and Crystallization Behavior in the $Pb_5Ge_3O_{11}$–$PbTiO_3$–$PbZrO_3$ Glass-Ceramic System," *Ferroelectrics*, **154**, 53–58 (1994).

[38]E. Breval, M. Hammond, and C. G. Pantano, "Nanostructural Characterization of Silicon Oxycarbide Glasses and Glass-Ceramics," *J. Am. Ceram. Soc.*, **77** [11] 3012–18 (1994).

[39]B. Houng and M. J. Haun, "Lead Zirconate Titanate–Lead Silicate Piezoelectric Glass-Ceramics," *Proc. IEEE Int. Symp. Appl. Ferroelectr.*, **94CH3416-5**, 214–17 (1994).

[40]W. Dressler and R. Riedel, "Progress in Silicon-Based Non-Oxide Structural Ceramics," *Int. J. Refract. Met. Hard Mater.*, **15**, 13–47 (1997).

[41]V. M. Sglavo, D. R. Maschio, G. D. Soraru, and A. Bellosi, "Fabrication of Polymer-Derived Si_2N_2O–ZrO_2 Nanocomposite Ceramics," *J. Mater. Sci.*, **28**, 6437–41 (1993).

[42]M. L. Balmer, H. Eckert, N. Das, and F. F. Lange, "^{27}Al Nuclear Magnetic Resonance of Glassy and Crystalline $Zr_{(1-x)}Al_xO_{(2-x/2)}$ Materials Prepared from Solution Precursors," *J. Am. Ceram. Soc.*, **79** [2] 321–26 (1996). □